

isomers: $\delta = 6.95-7.04$ (m, PPh_3), $7.15-7.28$ (m, $\text{NC}_9\text{H}_6\text{NH}$), $7.82-7.90$ (m, PPh_3); ^{13}C and ^{11}B NMR spectra were not obtained due to low solubility; IR (Nujol): $\tilde{\nu} [\text{cm}^{-1}] = 1902\text{vs}$ (CO); ^1H NMR shows 1.0 equiv of C_6H_6 present as solvent of crystallization; elemental analysis calcd for $\text{C}_{46}\text{H}_{37}\text{BCl}_2\text{N}_2\text{OOSp}_2 \cdot \text{C}_6\text{H}_6$: C 59.72, H 4.14, N 2.67; found: C 59.87, H 4.22, N 2.64.

2b: A solution of Bu_4NI (110 mg, 0.298 mmol) in CH_2Cl_2 (5 mL) was added to a suspension of **2a** (90 mg, 0.093 mmol) in CH_2Cl_2 (15 mL), and the resultant mixture stirred for 40 min to give a dark red solution. Reduction of the solvent volume to about 1 mL in vacuo and addition of hexane gave an orange solid. The solid was collected on a sintered glass crucible and washed with EtOH, toluene, and hexane to give pure **2b** as a deep purple solid. Yield 93 mg (94 %); ^1H NMR (400 MHz, CD_2Cl_2 , 25°C , TMS): major isomer: $\delta = 6.87$ (m, 1H, $\text{NC}_9\text{H}_6\text{NH}$), 7.52 (m, 1H, $\text{NC}_9\text{H}_6\text{NH}$), 8.25 (s, 1H, $\text{NC}_9\text{H}_6\text{NH}$), 8.40 (m, 1H, $\text{NC}_9\text{H}_6\text{NH}$), 8.46 (m, $\text{NC}_9\text{H}_6\text{NH}$), 8.65 (m, 1H, $\text{NC}_9\text{H}_6\text{NH}$); minor isomer: $\delta = 6.82$ (m, 1H, $\text{NC}_9\text{H}_6\text{NH}$), 7.23 (m, 1H, $\text{NC}_9\text{H}_6\text{NH}$), 7.49 (m, 1H, $\text{NC}_9\text{H}_6\text{NH}$), 8.27 (s, 1H, $\text{NC}_9\text{H}_6\text{NH}$), 8.57 (m, 1H, $\text{NC}_9\text{H}_6\text{NH}$), 10.11 (m, 1H, $\text{NC}_9\text{H}_6\text{NH}$); overlapping signals of both isomers: $\delta = 6.97-7.04$ (m, PPh_3), $7.29-7.35$ (m, $\text{NC}_9\text{H}_6\text{NH}$), $7.75-7.87$ (m, PPh_3); $^{13}\text{C}\{^1\text{H}\}$ NMR (100 MHz, CD_2Cl_2 , 25°C , TMS): major isomer: $\delta = 127.48$ (t'), $^{24}\text{J}(\text{C,P}) = 10$ Hz, $o\text{-PPh}_3$), 129.58 (s, $p\text{-PPh}_3$), 135.04 (t' , $^{3,5}\text{J}(\text{C,P}) = 10$ Hz, $m\text{-PPh}_3$); minor isomer: $\delta = 127.65$ (t' , $^{24}\text{J}(\text{C,P}) = 10$ Hz, $o\text{-PPh}_3$), 129.45 (s, $p\text{-PPh}_3$), 134.59 (t' , $^{3,5}\text{J}(\text{C,P}) = 10$ Hz, $m\text{-PPh}_3$); signals from other C atoms not observed due to low solubility; ^{11}B NMR (128 MHz, CD_2Cl_2 , 25°C , $\text{BF}_3 \cdot \text{OEt}_2$): $\delta = 51.7$; IR (Nujol): $\tilde{\nu} [\text{cm}^{-1}] = 1909\text{m}$, 1892s , 1876s (CO); UV/Vis (CH_2Cl_2): $\lambda_{\text{max}} = 521.5$ nm; elemental analysis for $\text{C}_{46}\text{H}_{37}\text{BClIN}_2\text{OOSp}_2$: calcd: C 52.17, H 3.52, N 2.65; found: C 52.42, H 3.69, N 2.73.

Received: October 18, 1999 [Z14151]

- [1] a) H. Wadeppohl, *Angew. Chem.* **1997**, *109*, 2547–2550; *Angew. Chem. Int. Ed. Engl.* **1997**, *36*, 2441–2444; b) H. Braunschweig, *Angew. Chem.* **1998**, *110*, 1882–1898; *Angew. Chem. Int. Ed.* **1998**, *37*, 1786–1801; c) G. J. Irvine, M. J. G. Lesley, T. B. Marder, N. C. Norman, C. R. Rice, E. G. Robins, W. R. Roper, G. R. Whittell, L. J. Wright, *Chem. Rev.* **1998**, *98*, 2685–2722; d) M. R. Smith, III, *Prog. Inorg. Chem.* **1999**, *48*, 505–567.
- [2] a) H. Braunschweig, C. Kollann, U. Englert, *Angew. Chem.* **1998**, *110*, 3355–3357; *Angew. Chem. Int. Ed.* **1998**, *37*, 3179–3180; b) A. H. Cowley, V. Lomeli, A. Voigt, *J. Am. Chem. Soc.* **1998**, *120*, 6401–6402; c) B. Wrackmeyer, *Angew. Chem.* **1999**, *111*, 817–818; *Angew. Chem. Int. Ed.* **1999**, *38*, 771–772.
- [3] A. W. Ehlers, E. J. Baerends, F. M. Bickelhaupt, U. Radius, *Chem. Eur. J.* **1998**, *4*, 210–221.
- [4] a) H. Braunschweig, T. Wagner, *Angew. Chem.* **1995**, *107*, 904–905; *Angew. Chem. Int. Ed. Engl.* **1995**, *34*, 825–826; b) M. Shimoi, S. Ikubo, Y. Kawano, K. Katoh, H. Ogino, *J. Am. Chem. Soc.* **1998**, *120*, 4222–4223.
- [5] a) T. D. Tilley in *The Silicon–Heteroatom Bond* (Eds.: S. Patai, Z. Rappoport), Wiley, New York, **1991**, Chaps. 9 and 10; b) C. Zybill, *Adv. Organomet. Chem.* **1994**, *36*, 229–281; c) P. D. Lickiss, *Chem. Soc. Rev.* **1992**, 271–279; d) K. Ueno, H. Tobita, M. Shimoi, H. Ogino, *J. Am. Chem. Soc.* **1988**, *110*, 4092–4093.
- [6] a) G. J. Irvine, W. R. Roper, L. J. Wright, *Organometallics* **1997**, *16*, 2291–2296; b) C. E. F. Rickard, W. R. Roper, A. Williamson, L. J. Wright, *Organometallics* **1998**, *17*, 4869–4874.
- [7] Data for the X-ray structure analyses: **2b**: crystals from dichloromethane/benzene; $\text{C}_{46}\text{H}_{37}\text{BClIN}_2\text{OOSp}_2 \cdot 0.5 \text{C}_6\text{H}_6$, $M_r = 1098.13$; crystal dimensions $0.28 \times 0.25 \times 0.08$ mm; monoclinic; space group $\text{C}2/c$; $a = 30.0757(4)$, $b = 20.6367(2)$, $c = 17.1417(2)$ Å, $\beta = 111.176(1)^\circ$, $Z = 8$, $V = 9920.8(2)$ Å³, $\rho_{\text{calcd}} = 1.470$ g cm^{−3}; $T = 203$ K; $2\theta_{\text{max}} = 55^\circ$; of 30013 total reflections, 10794 were unique ($R_{\text{int}} = 0.0259$); Siemens SMART CCD diffractometer, $\text{MoK}\alpha$ radiation ($\lambda = 0.71073$ Å); empirical absorption correction ($\mu = 3.346$ mm^{−1}, $T_{\text{min}}/T_{\text{max}} = 0.454/0.775$). The structure was solved by Patterson methods and refined by full-matrix least-squares on F^2 on all data. The asymmetric unit cell contains one molecule of **2b**, in which the chloro and carbonyl ligands are disordered equally between the two sites, and half a molecule of benzene. $R_1 =$

0.0518 for the 8660 observed data ($I > 2\sigma(I)$) and $wR_2 = 0.1712$ for all data. Goodness of fit on F^2 1.078. **3**: crystals from dichloromethane/toluene/*n*-hexane; $\text{C}_{48}\text{H}_{42}\text{BClN}_2\text{O}_2\text{OsP}_2 \cdot \text{C}_7\text{H}_8$, $M_r = 1069.37$; crystal dimensions $0.40 \times 0.28 \times 0.22$ mm; monoclinic; space group $P2_1/n$; $a = 16.6920(2)$, $b = 17.7366(1)$, $c = 17.6239(2)$ Å, $\beta = 106.510(1)^\circ$, $Z = 4$, $V = 5002.65(9)$ Å³, $\rho_{\text{calcd}} = 1.420$ g cm^{−3}; $T = 200$ K; $2\theta_{\text{max}} = 54^\circ$; of 29951 total reflections, 10719 were unique ($R_{\text{int}} = 0.0220$); Siemens SMART CCD diffractometer, $\text{MoK}\alpha$ radiation ($\lambda = 0.71073$ Å); empirical absorption correction ($\mu = 2.708$ mm^{−1}, $T_{\text{min}}/T_{\text{max}} = 0.410/0.587$). The structure was solved by Patterson and Fourier methods and refined by full-matrix least-squares on F^2 on all data. The asymmetric unit cell contains one molecule of **3** and one molecule of toluene; $R_1 = 0.0247$ for the 9473 observed data ($I > 2\sigma(I)$) and $wR_2 = 0.0630$ for all data. Goodness of fit on F^2 1.053. Programs used: SHELXS-97 (structure solution) and SHELXL-97 (structure refinement). Crystallographic data (excluding structure factors) for the structures reported in this paper have been deposited with the Cambridge Crystallographic Data Centre as supplementary publication nos. CCDC-135052 (**2b**) and CCDC-135053 (**3**). Copies of the data can be obtained free of charge on application to CCDC, 12 Union Road, Cambridge CB2 1EZ, UK (fax: (+44) 1223 336 033; e-mail: deposit@ccdc.cam.ac.uk).

[8] Longest of the 629 determinations found in the CCSD.

[9] t' denotes that the signal has apparent multiplicity; $^{n,m}\text{J}(\text{C,P})$ is the sum of the two coupling constants $^n\text{J}(\text{C,P})$ and $^m\text{J}(\text{C,P})$, as explained in S. M. Maddock, C. E. F. Rickard, W. R. Roper, L. J. Wright, *Organometallics* **1996**, *15*, 1793–1803.

Orientation-Controlled Monolayer Assembly of Zeolite Crystals on Glass and Mica by Covalent Linkage of Surface-Bound Epoxide and Amine Groups**

Alexander Kulak, Yun-Jo Lee, Yong Soo Park, and Kyung Byung Yoon*

Efforts have been made during the last decade to develop zeolite thin films for separative, catalytic, and chemical sensor applications.^[1–10] For practical purposes, they have usually been prepared on various substrates or supports since they are extremely fragile. The chemical methods to assemble zeolite thin films on substrates can generally be classified into two groups, namely, “direct growth”^[1–5] and “postsynthetic crystal attachment”.^[6, 7] The former group usually involves in situ growth of the zeolite crystals or films on the substrates by immersing them into the synthesis gel.^[1–4] For best results, the substrates are often chemically modified or pretreated with colloidal seed crystals. The unique pulsed laser ablation of preformed supported zeolites can also be classified into this group.^[5] In the latter group, preformed zeolite crystals are chemically attached on substrates by ionic or covalent bonding by use of appropriate organic additives.^[6, 7] For these

[*] Prof. Dr. K. B. Yoon, Dr. A. Kulak, Dr. Y.-J. Lee, Dr. Y. S. Park
Center for Microcrystal Assembly
Department of Chemistry
Sogang University
Seoul 121-742 (Korea)
Fax: (+82) 2-706-4269
E-mail: yoonkb@ccs.sogang.ac.kr

[**] We thank the Ministry of Science and Technology, Korea, for financial support through the Creative Research Initiatives Program.

methods, the organic functional groups are usually tethered onto either the zeolites or the substrates by covalent bonding, proceeded by subsequent chemical linkage between the tethered functional groups and the unmodified surface. However, the coverage and orientation of the zeolite crystals attached onto the substrates by this “one-component modification” were rather poor. In fact, the ability to uniformly align zeolite crystals on substrates during the assembly is essential for the applications of zeolite thin films as the hosts for quantum dots, magnetic particles, nonlinear optical materials,^[8, 9] or chemical sensors.^[11] It has been reported that zeolite crystals tend to physically adhere onto substrates with their flat faces facing the substrate when the substrate is dip coated into a colloidal zeolite solution.^[2] This phenomenon led to uniform alignment of cubic zeolite A crystals on substrates with a face parallel to the plane of the substrate.^[2] For zeolites with lower symmetry, particularly for those that possess significant net intrinsic dipole moments due to one of the axes being longer than the other two, the application of strong electric fields is highly effective in aligning the crystals with the longest axis parallel to the direction of the electric field.^[10] We now report a novel “two-component modification” strategy that leads to monolayer assembly of zeolite A and ZSM-5 crystals onto glass and mica with very high surface coverage and also uniform alignment. This new approach involves independent tethering of two different functional groups onto the zeolite and the substrate, followed by covalent linking of the two tethered functional groups as schematically illustrated in Scheme 1.

Visual observation of the zeolite-coated glass plate prepared by the method shown in Scheme 1 revealed that the entire glass plate (18 × 18 mm) was uniformly covered with white zeolite A crystals. A thin layer of zeolite particles maintained adhesion onto the glass substrate even after sonication for 30 s in toluene. Omitting the surface anchoring of any of the silyl compounds in the binding procedure resulted in essentially empty glass plates scarcely covered with physisorbed zeolite crystals; these few crystals immediately fell off the glass plate during sonication. This result strongly indicates that facile formation of amine–hydroxide bridges indeed proceeds between terminal amine and epoxide groups, which leads to effective assembly of zeolite A crystals on the

glass substrate. The efficacy of uniform coverage of the entire glass surface seemed to depend on factors such as the uniformity of the chemical composition, the pretreatment of the glass substrate, the degree of coverage of the corresponding organic compound on the glass and zeolite, and the size and morphology of the zeolite crystals.

The scanning electron micrograph (SEM) of the glass plate coated with zeolite A crystals revealed that almost the entire plate was covered by the zeolite crystals with high-density packing, as shown in Figure 1 A. Observation at a higher

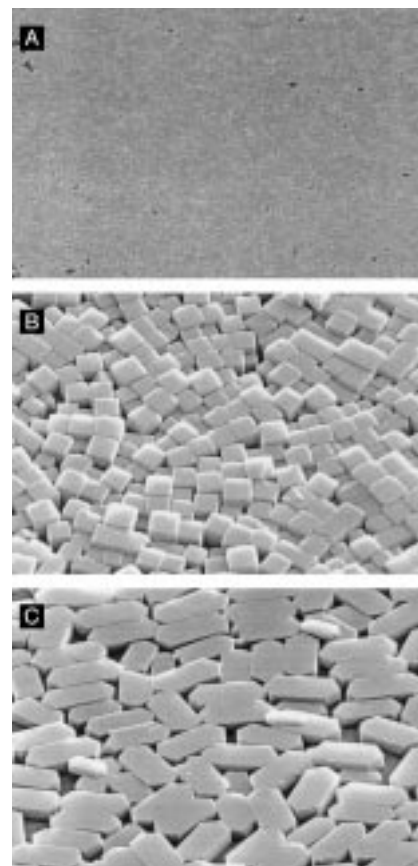
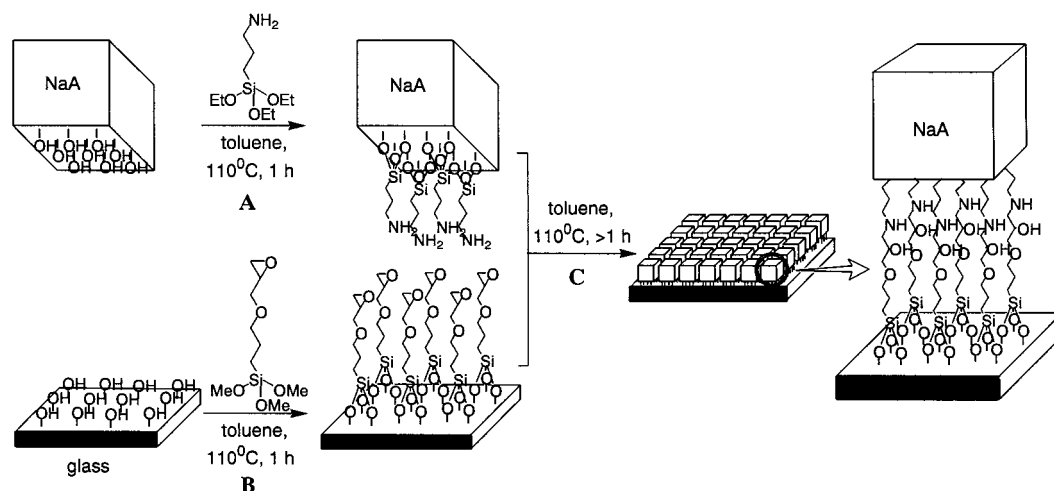


Figure 1. Scanning electron micrographs showing the monolayers of zeolite A crystals bound to a glass substrate at magnifications of × 200 (A) and × 12 000 (B), and ZSM-5 crystals at a magnification of × 5 000 (C).



Scheme 1. The procedure to assemble zeolite A monolayer on a glass substrate.

magnification (Figure 1 B) revealed that only a monolayer of the crystals was assembled on the glass. Moreover, this image shows the striking feature that all the zeolite crystals are aligned with a face parallel to the glass substrate, a perfect one-dimensional orientation.

Most interestingly, the zeolite A crystals showed a strong tendency to pack closely during the attachment onto the substrate with the side faces in contact. This phenomenon indicates that a 3-aminopropyl-covered zeolite A crystal, once mounted on the substrate, tends to act as a template for positioning the next crystal. Although further study is necessary, we propose for the moment that such a close packing arises due to a strong face-to-face interaction between the 3-aminopropyl-covered faces of two separate zeolite A crystals through a large number of hydrogen bonds between the terminal NH_2 groups. Consistent with our proposal, the commonly observed close packing of the physisorbed, unmodified zeolite crystals on substrates during dip coatings has also been attributed to hydrogen bonding between the surface hydroxyl groups of zeolites.^[2]

Figure 1 C shows the SEM image of a monolayer of ZSM-5 crystals similarly assembled on a glass substrate. This figure demonstrates that the method described above works equally well even for large ($\approx 5 \mu\text{m}$) zeolite crystals. This image further shows that all the ZSM-5 crystals assemble with their b axis perpendicular to the glass surface despite that the rectangular-shaped side faces can, in principle, also be attached onto the surface. This preferential orientation might occur because ZSM-5 crystals can have better contact with the glass substrate through their substantially larger $[010]$ face than through their smaller side faces. It was also noticed that the intercrystalline void spaces increase upon changing from zeolite A to ZSM-5, presumably due to the lower symmetry and increased size of ZSM-5 relative to zeolite A. The orthorhombic CoAPO-34 and SAPO-34 molecular sieve crystals ($\approx 7 \mu\text{m}$) also efficiently assembled onto the glass substrate with similar high-density, monolayer packing by the same method. The SEM images of the assembled molecular sieves (not shown) revealed that these crystals also align with a face parallel to the substrate. However, no preference for a particular face for these crystals was observed, presumably due to less substantial differences in the area of the three faces. The attachment method was also effective for freshly cut mica as the substrate, although the coverage was usually a bit less than onto glass.

The XRD pattern of the zeolite A-coated glass showed only five lines that correspond to $[200]$, $[600]$, $[800]$, $[1000]$, and $[1200]$ planes of the zeolite A crystals (Figure 2a). The reflection for $[400]$ expected at $2\theta = 14.40^\circ$ seems to be lost in the background due to an intrinsically very low intensity (less than 0.5% of the $[200]$ reflection).^[12] Such a simple pattern contrasts strongly with the more common, complex pattern of the randomly oriented zeolite A crystal powder shown in the inset. Likewise, only five lines appeared from the monolayer of ZSM-5 crystals due to $[020]$, $[040]$, $[060]$, $[080]$, and $[0100]$ reflections (Figure 2b).

The strength of bonding between zeolite A crystals and substrates seems to vary and is sensitively dependent on the assembly procedure. That a large number of zeolite A crystals

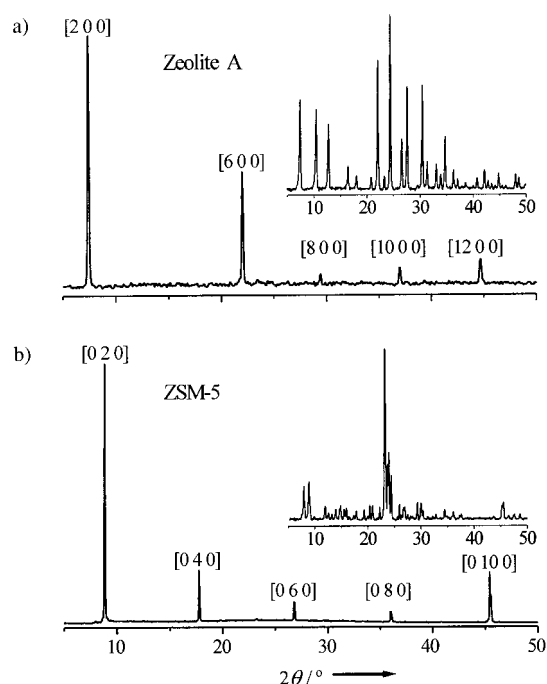


Figure 2. X-ray powder diffraction patterns of a) zeolite A and b) ZSM-5 monolayers showing the aligned state of crystals on glass substrates. Insets: XRD patterns for randomly oriented powders of the zeolites.

remain adhered to the glass substrate even after sonication as long as 5 min suggests the bonding to be fairly strong. Interestingly, SEM images of the extensively sonicated samples revealed that most of the surviving zeolite particles had become severely fractured. This result contrasts with the fact that all the zeolite A particles retain their original cubic morphology under the same treatment conditions as a free powder. The larger ZSM-5, CoAPO-34, and SAPO-34 crystals tend to be more easily removed by sonication.

This report introduces a novel strategy to assemble monolayers of zeolite A and ZSM-5 onto glass and mica substrates with a perfect one-dimensional orientation through covalent binding between two independently tethered, terminal functional groups, in this case epoxide and amine. This method uniquely provides strong zeolite–substrate bonding, high surface coverage, uniform orientation, and easy control of the monolayer assembly. In a broader sense, this report demonstrates a novel strategy to efficiently organize micrometer-sized nanoporous inorganic crystals into functional macroscopic structure.

Experimental Section

Zeolite A, ZSM-5, CoAPO-34, and SAPO-34 were synthesized according to the literature procedures. The synthetic templates were not removed from the zeolite or molecular sieve crystals prior to assembly. The washed and dried zeolite or molecular sieve (0.2 g) was treated with 3-aminopropyltriethoxysilane (2 mm, 10 mL, 110°C , 1 h) under argon. This led to 3-aminopropylsilyl groups covalently bound onto the zeolite or molecular sieve surface (see Scheme 1A). The presence of the surface-bound 3-aminopropylsilyl groups was confirmed by purple coloration of the surface when treated with 1,2,3-triketohydrindene (ninhydrin) at room temperature.^[13] The diffuse-reflectance UV/Vis spectrum of the purple-coloured zeolite showed an adsorption at 570 nm indicating the formation of diketohydrindylidenediketohydrinamine. Control experiments with

fresh zeolites undoped with aminopropylsilyl groups did not develop the characteristic purple color.

Independently, a piece of thin glass ($18 \times 18 \text{ mm}^2$) was treated with [3-(2,3-epoxypropoxy)propyl]trimethoxysilane (2 mm) in toluene (10 mL, 110°C , 1 h) under argon to assemble a layer of 3-(2,3-epoxypropoxy)propylsilyl groups on the glass surface (see Scheme 1B). The presence of surface-bound terminal epoxy groups attached on the glass was confirmed by pale-red coloration of the surface when treated with an aminated azo dye (Fat Brown RR) at 110°C in toluene.^[14] The UV/Vis spectrum of the glass showed a broad band with the absorption maximum at $\approx 440 \text{ nm}$. Undoped glasses gave negligible intensities in the $\approx 440 \text{ nm}$ region.

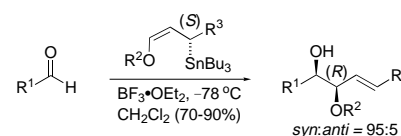
The coated glass plate was inserted into a suspension of 3-aminopropylsilyl-coated zeolite powders in toluene (0.1 g, 10 mL) and the mixture was refluxed ($> 1 \text{ h}$) under argon (see Scheme 1C). The zeolite-coated opaque glass was then removed from the reaction mixture and washed extensively with toluene. The zeolite-coated glass was subsequently sonicated in toluene for 20 s to remove physisorbed zeolite crystals on the chemically bound first layer.

Received: July 12, 1999 [Z13716]

Addition of Enantioenriched γ -Oxygenated Allylic Stannanes to *N*-Acyl Iminium Intermediates: A New Synthesis of *syn*-Amino Alcohol Derivatives**

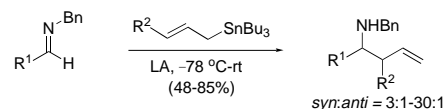
James A. Marshall,* Kevin Gill, and Boris M. Seletsky

Some years ago we discovered a facile route to mono-protected *syn*-1,2-diol derivatives through BF_3 -promoted addition of enantioenriched γ -oxygenated allylic stannanes to aldehydes (Scheme 1).^[1] We had hoped to extend these



Scheme 1. A facile route to monoprotected *syn*-1,2-diol derivatives. R^1 = alkyl, alkenyl; R^2 = methoxymethyl (MOM), tributylsilyl (TBS), benzyl-oxymethyl (BOM); R^3 = alkyl.

additions to imines, along the lines reported by Keck and Enholm (Scheme 2),^[2] but were unsuccessful in these attempts. No detectable β -amino ether adducts were formed, even at room temperature. We attributed these failures to the lower reactivity of oxygenated allylic stannanes relative to their nonoxygenated allyl and crotyl counterparts.^[3]



Scheme 2. Addition of allylic stannanes to imines. R^1 = $c\text{-C}_6\text{H}_{11}$, Ph, $s\text{Bu}$, $i\text{Pr}$; R^2 = H, Me; Lewis acid LA = $\text{BF}_3 \cdot \text{OEt}_2$, TiCl_4 . Bn = benzyl, rt = room temperature.

A report by Yamamoto and Schmid, describing the addition of a γ -OMOM allylic stannane to several *N*-acyliminium intermediates from Hiemstra and Speckamp^[4] (Scheme 3), prompted our examination of this alternative route to β -amino alcohol derivatives.^[5] In fact, addition of the racemic (*Z*)- γ -oxygenated allylic stannanes **2a** and **2b**^[1] to the *N*-acyliminium precursor **1**, derived from isovaleraldehyde,^[5] proceeded in high yield to afford the desired adducts (Table 1). Unfortunately, a mixture of *syn* and *anti* isomers **3** and **4** was obtained from these additions.

[*] Prof. J. A. Marshall, K. Gill
Department of Chemistry
University of Virginia
Charlottesville, VA 22904 (USA)
Fax: (+1) 804-924-7993
E-mail: jam5x@virginia.edu
Dr. B. M. Seletsky
Eisai Research Institute
4 Corporate Drive, Andover, MA 01910 (USA)

[**] This research was supported by the National Institute of Allergy and Infectious Diseases (grant R01 AI31422).

Supporting information for this article is available on the WWW under <http://www.wiley-vch.de/home/angewandte/> or from the author.

- [1] a) S. Feng, T. Bein, *Nature* **1994**, 368, 834–836; b) S. Feng, T. Bein, *Science* **1994**, 265, 1839–1841.
- [2] a) A. Gouzinis, M. Tsapatsis, *Chem. Mater.* **1998**, 10, 2497–2504; b) L. C. Boudreau, J. A. Kuck, M. Tsapatsis, *J. Membr. Sci.* **1999**, 152, 41–59, and references therein.
- [3] S. Mintova, J. Hedlund, B. Schoeman, V. Valtchev, J. Sterte, *Chem. Commun.* **1997**, 15–16.
- [4] a) G. Clet, J. C. Jansen, H. van Bekkum, *Chem. Mater.* **1999**, 11, 1696–1702; b) N. van der Puil, F. M. Dautzenberg, H. van Bekkum, J. C. Jansen, *Microporous Mesoporous Mater.* **1999**, 27, 95–106, and references therein.
- [5] a) T. Munoz, Jr., K. J. Balkus, Jr., *Chem. Mater.* **1998**, 10, 4114–4122; b) T. Munoz, Jr., K. J. Balkus, Jr., *J. Am. Chem. Soc.* **1999**, 121, 139–146.
- [6] a) Y. Yan, T. Bein, *J. Am. Chem. Soc.* **1995**, 117, 9990–9994; b) Y. Yan, T. Bein, *J. Phys. Chem.* **1992**, 96, 9387–9393; c) T. Bein, *Chem. Mater.* **1996**, 8, 1636–1653.
- [7] Z. Li, C. Lai, T. E. Mallouk, *Inorg. Chem.* **1989**, 28, 178–182.
- [8] a) G. A. Ozin, A. Kuperman, A. Stein, *Angew. Chem. Adv. Mater.* **1989**, 101, 373–390; *Angew. Chem. Int. Ed. Engl. Adv. Mater.* **1989**, 28, 359–376; *Adv. Mater.* **1989**, 1, 69–86; b) G. A. Ozin, *Adv. Mater.* **1992**, 4, 612–650.
- [9] G. D. Stucky, J. E. MacDougall, *Science* **1990**, 247, 669–678.
- [10] a) J. Caro, G. Finger, J. Kornatowski, *Adv. Mater.* **1992**, 4, 273–276; b) J. Caro, M. Noack, J. Richter-Mendau, F. Marlow, D. Petersohn, M. Griepentrog, J. Kornatowski, *J. Phys. Chem.* **1993**, 97, 13685–13690; c) M. Noack, P. Kölsch, D. Venzke, P. Toussaint, J. Caro, *Microporous Mater.* **1994**, 3, 201–206; d) P. Kölsch, D. Venzke, M. Noack, E. Lieske, P. Toussaint, J. Caro, *Stud. Surf. Sci. Catal.* **1994**, 84, 1075–1082.
- [11] C. Plog, W. Maunz, P. Kurzweil, E. Obermeier, C. Scheibe, *Sens. Actuators* **1995**, 24–25, 403–406.
- [12] Due to this low intensity, this reflection is usually not observed even from the corresponding powder diffraction patterns as noticed in the inset. See: M. M. J. Treacy, J. B. Higgins, R. von Ballmoos, *Collection of Simulated XRD Powder Patterns for Zeolites*, 3rd ed., International Zeolite Association, Zürich, **1996**, pp. 500–503.
- [13] a) S. Sheng, J. J. Kraft, S. M. Schuster, *Anal. Biochem.* **1993**, 211, 242–249; b) P. J. Lamothe, P. G. McCormic, *Anal. Chem.* **1973**, 45, 1906–1911.
- [14] J. D. Godfrey, Jr., E. M. Gordon, D. J. Von Langen, *Tetrahedron Lett.* **1987**, 28, 1603–1606.